

A High-Efficiency RF Harvester with Maximum Power Point Tracking [†]

Manel Gasulla ^{1,*}, Francesc J. Robert ¹, Josep Jordana ¹, Edgar Ripoll-Vercellone ^{1,2}, Jordi Berenguer ³ and Ferran Reverter ¹

¹ e-CAT Group, Department of Electronic Engineering, Universitat Politècnica de Catalunya, 08860 Castelldefels, Spain; francesc.j.robert@upc.edu (F.J.R.); jose.jordana@upc.edu (J.J.); edgar.ripoll.vercellone@upc.edu (E.R.-V.); ferran.reverter@upc.edu (F.R.)

² Idneo Technologies, 08100 Mollet del Vallès, Spain

³ CSC Group, Department of Signal Theory and Communications, Universitat Politècnica de Catalunya, 08860 Castelldefels, Spain; jordi.berenguer@upc.edu

* Correspondence: manel.gasulla@upc.edu; Tel.: +34-934137092

[†] Presented at the Eurosensors 2018 Conference, Graz, Austria, 9–12 September 2018.

Published: 23 November 2018

Abstract: This paper presents the implementation of a high-efficiency radiofrequency (RF) harvester, which consists of a rectenna and a maximum power point tracker (MPPT). The rectenna was characterized from -30 dBm to -10 dBm at 808 MHz, achieving an efficiency higher than 60% at -10 dBm. Experimental results also show that the rectenna can be well modelled as a Thévenin equivalent circuit, which allows the use of a simple ensuing MPPT. The complete RF harvester was tested, achieving an overall efficiency near 50% at -10 dBm. Further tests were performed powering a sensor node from a nearby antenna.

Keywords: RF harvesting; rectenna; MPPT; sensor nodes

1. Introduction

RF energy harvesting has been extensively proposed to power tiny devices such as RFID or IoT (Internet of Things) nodes [1–4]. RF energy can be harvested either from dedicated sources or from the RF energy already present in the ambient and coming from unintentional sources. Figure 1 shows the generic block diagrams of: (a) an RF harvester powering a sensor node, and (b) a sensor node. The rectenna transforms the RF signal to a dc voltage and the MPPT provides the optimum load to the rectenna in order to transfer maximum power to the sensor node.

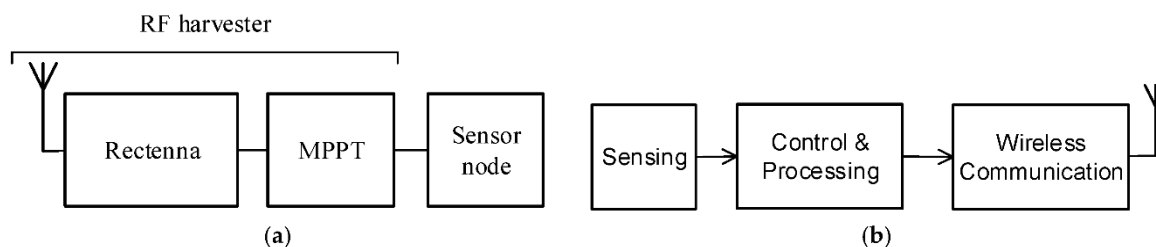


Figure 1. Generic block diagrams of: (a) an RF harvester; (b) a sensor node.

This paper continues and complements the work presented in [5] in two ways. First, the rectenna is fully characterized and modelled as a Thévenin equivalent circuit. Secondly, an MPPT is added to automatically operate at the maximum power point (MPP) of the rectenna. At an input power of -10

dBm, the efficiencies of both the rectenna and the MPPT are high, achieving an overall efficiency around 50%. As an application example, the RF harvester is used to power a sensor node that forms part of a smart gas meter [6].

2. RF Harvester

Figure 2a shows the schematic circuit of the rectenna, which includes an antenna, a high-pass L-matching network (composed of a capacitor C_m and an inductor L_m), a half-wave rectifier and an output filtering capacitor (C_o). The antenna is modelled as a sinusoidal voltage source v_a in series with a radiation resistance R_a and provides a power P_{av} at matching conditions. The parameters V_o , I_o , and P_o are the DC voltage, current, and power at the rectenna output, respectively. An equivalent resistance R_o is defined as V_o/I_o .

The rectenna output can be modelled as a Thévenin equivalent (a dc voltage source V_{oc} in series with a resistance R_T), such as in Figure 2b. The calculus of the Thévenin parameters is simple assuming no losses in the components and the diode [7] but otherwise is rather complex [2]. On the other hand, the parameters can be inferred by experimental characterization [3], which will be the strategy followed here. According to this model and to the maximum power transfer theorem, maximum power will be achieved when the ensuing stage presents an equivalent input resistance $R_o = R_T$, which implies $V_o = 0.5V_{oc}$.

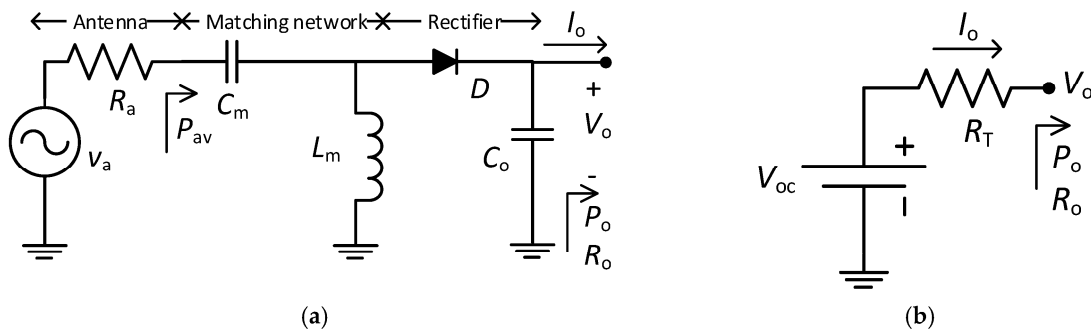


Figure 2. Rectenna: (a) Schematic circuit; (b) Thévenin equivalent circuit.

In general, a sensor node directly connected to the output of the rectenna will not accomplish that condition and an intermediate stage, such as an MPPT, has to be used. An MPPT mainly consists of a DC/DC converter and a tracking algorithm. In particular, the fractional open circuit voltage (FOCV) technique leads to simple power-efficient implementations. In this technique, the open circuit voltage, V_{oc} in Figure 2b, of the energy transducer is first measured and a fraction k of V_{oc} is used in order to fix V_o to the MPP voltage, V_{MPP} . Assuming the model of Figure 2b, $k = 0.5$ is the proper choice and thus $V_{MPP} = 0.5V_{oc}$. Figure 3 illustrates the block diagram for an implementation of the FOCV-MPPT technique, where P_{load} is the power transferred to the sensor node. The operation is the following. First, S_1 is closed and S_2 is open (sampling period). For high values of R_{oc1} and R_{oc2} , the output of the rectenna can be considered as open and thus $V_o = V_{oc}$. The voltage divider formed by R_{oc1} and R_{oc2} fixes $V_{MPP} = kV_{oc}$. The input capacitor C_L momentarily stores the incoming harvested energy. Secondly, S_1 is open and S_2 is closed (regulation period). Thus, V_{MPP} holds constant thanks to C_{REF} , and the DC/DC converter settles V_o around V_{MPP} and transfers the harvested energy by the rectenna to the node. In order to increase the efficiency at light loads, the DC/DC converter uses special control regulation techniques such as pulse-frequency modulation (PFM) or burst-mode [8].

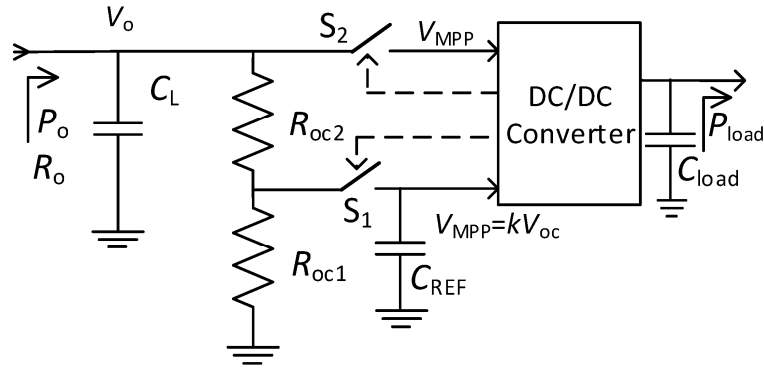


Figure 3. Block diagram of an implementation of the FOCV-MPPT technique.

3. Materials and Methods

The rectenna presented in [5] was used here. It consists of a printed circuit board with Rogers substrate and the following components: $C_m = 0.5$ pF (AVX), $C_o = 1$ nF, $L_m = 27$ nH (Coilcraft), and a Schottky HSMS-2850 diode (Avago Technologies). The circuit of Figure 2a was used for its characterization, where an RF generator (Agilent E4433B) is connected at the input instead of the antenna and a Source-Measure Unit (SMU, Agilent B2901A) configured as a voltage sink (quadrant IV) at the output. The generator was set at a tuned optimal frequency of 808 MHz and at P_{av} of -30 dBm, -20 dBm, and -10 dBm. For each value of P_{av} , the SMU was set at different values of V_o while measuring P_o . Then, η_{rect} was obtained as P_o/P_{av} .

As for the FOCV-MPPT, a BQ25504 chip (Texas Instruments) was used, and in particular an evaluation board from the manufacturer. The chip contains a boost converter with PFM control and the board includes $C_L = 4.8$ μ F and $C_{load} = 104.8$ μ F. The default values of R_{oc1} and R_{oc2} were modified to 10 M Ω in order to fix $k = 0.5$ (by default 0.78). The sampling and regulation periods are prefixed to 256 ms and 16 s, respectively. Then, the efficiency of the whole RF harvester (rectenna plus MPPT) was characterized by using the RF generator at the input of the rectenna and the SMU set at 3 V at the output of the MPPT. The overall efficiency, η_T , was calculated as P_{load}/P_{av} . The efficiency of the MPPT, η_{MPPT} , was not directly measured but can be inferred from

$$\eta_T = \eta_{rect,max} \eta_{MPPT}, \quad (1)$$

where $\eta_{rect,max}$ is η_{rect} at the MPP.

A setup was also used to power a sensor node with the RF harvester. The selected sensor node is used to upgrade a mechanical gas meter to a smart device [6]. For the tests, the node was programmed to stay in a standby mode, consuming about 1.4 μ A. The input power (P_{av}) was set to keep the voltage supply of the sensor node around 3 V, thus $P_{load} \approx 4.2$ μ W. The required value of P_{av} can be estimated from

$$P_{load} = \eta_T P_{av}. \quad (2)$$

As for the RF harvester input, two configurations were used: (1) an RF generator and (2) a receiving monopole antenna. In the second case, another identical monopole antenna was connected to a nearby RF generator, jointly acting as a wireless energy transmitter. The antennas showed an insertion loss higher than 10 dB at 808 MHz.

4. Experimental Results and Discussion

Figure 4a shows the experimental values of η_{rect} (in dots) versus V_o for the three values of P_{av} together with least-squares fits (continuous lines) corresponding to a Thévenin equivalent model such as that of Figure 2b. The continuous lines show good agreement with the experimental data, thus validating the Thévenin model. Table 1 shows for each value of P_{av} , the inferred Thévenin parameters R_T and V_{oc} , the achieved $\eta_{rect,max}$ and its corresponding voltage ($V_{MPP,exp}$), and the experimental open circuit voltage ($V_{oc,exp}$) of the rectenna. In Figure 4a, $\eta_{rect,max}$, $V_{MPP,exp}$, and $V_{oc,exp}$ are

also marked for $P_{av} = -10$ dBm. Achieved efficiencies ($\eta_{rect,max}$) are among the highest published in the literature for similar designs [5]. On the other hand, V_{oc} (the Thévenin voltage) nearly matches $V_{oc,exp}$. Finally, $V_{MPP,exp}$ equates or nearly matches $0.5V_{oc,exp}$, the regulated voltage at the input of the MPPT. Thus, the MPPT will be able to extract the maximum power (or nearly) from the rectenna.

Figure 4b shows the experimental values of η_T versus P_{av} . At -20 dBm, $\eta_{rect,max} = 39.3\%$ but $\eta_T = 6.5\%$, resulting, from (1), in $\eta_{MPPT} = 16.5\%$. This low value of η_{MPPT} is due to both a low input voltage value (140 mV = $0.5V_{oc,exp}$) and a low value of P_o (≈ 3.9 μ W = $\eta_{rect,max}P_{av}$). Contrariwise, at -10 dBm, $\eta_{rect,max} = 60.3\%$ and $\eta_T = 48.6\%$, resulting in $\eta_{MPPT} = 80.6\%$. At higher values of P_{av} (-5 dBm) η_T reached a value of 55.6% . Compared to [4], where a similar chip for the MPPT is used, η is quite higher.

When powering the sensor node, the required value of P_{av} was -17.6 dBm. This value fits well with (2), considering the corresponding efficiency in Figure 4b ($\approx 24\%$). This performance was also tested with the antennas at a distance of 0.5 m and 1 m. The power output of the remote RF generator was tuned at appropriate values in order to operate the node, resulting in 8.0 dBm and 13.2 dBm, respectively. These values accounted for the respective link budgets.

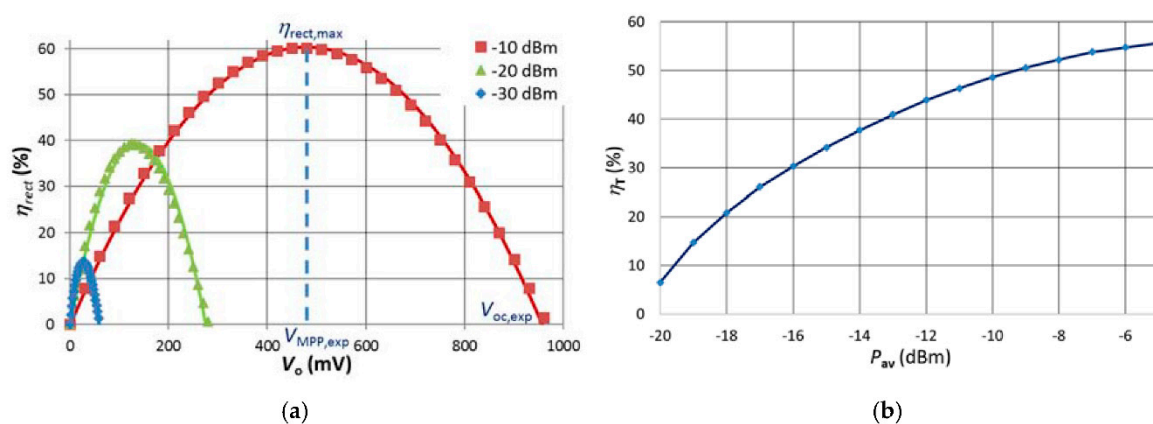


Figure 4. (a) η_{rect} versus V_o for different values of P_{av} . Continuous lines are least-squares fits corresponding to a Thévenin equivalent circuit; (b) η_T versus P_{av} .

Table 1. Inferred and measured parameters from the data of Figure 4a.

P_{av}/dBm	$R_T/\text{k}\Omega$	V_{oc}/mV	$\eta_{rect,max}/\%$	$V_{MPP,exp}/\text{mV}$	$V_{oc,exp}/\text{mV}$
-10	3.80	958	60.3	480	960
-20	4.79	275	39.3	130	280
-30	6.29	58.7	13.6	27	60

Acknowledgments: The authors thank Castelldefels School of Telecommunications and Aerospace Engineering for the RF instrumentation needed to perform the experiments. This work was supported by the Spanish State Research Agency (AEI) and by the European Regional Development Fund under Project TEC2016-76991-P.

Conflicts of Interest: The authors declare no conflict of interest. The founding sponsors had no role in the design of the study; in the collection, analyses, or interpretation of data; in the writing of the manuscript, and in the decision to publish the results.

References

1. Piñuela, M.; Mitcheson, P.D.; Lucyszyn, S. Ambient RF energy harvesting in urban and semi-urban environments. *IEEE Trans. Microw. Theory Tech.* **2013**, *61*, 2715–2726.
2. de Carli, L.G.; Juppa, Y.; Cardoso, A.J.; Galup-Montoro, C.; Schneider, M.C. Maximizing the Power Conversion Efficiency of Ultra-Low-Voltage CMOS Multi-Stage Rectifiers. *IEEE Trans. Circuits Syst. I Regul. Pap.* **2015**, *62*, 967–975.
3. Marian, V.; Allard, B.; Vollaïre, C.; Verdier, J. Strategy for Microwave Energy Harvesting from Ambient Field or a Feeding Source. *IEEE Trans. Power Electron.* **2012**, *27*, 4481–4491.

4. Talla, V.; Kellogg, B.; Ransford, B.; Naderiparizi, S.; Gollakota, S.; Smith, J.R. Powering the Next Billion Devices with Wi-Fi. ArXiv:1505.06815 [cs.NI] 2015. Available online: <https://arxiv.org/abs/1505.06815> (accessed on 22th November 2018).
5. Gasulla, M.; Jordana, J.; Robert, F.J.; Berenguer, J. Analysis of the optimum gain of a high-pass L-matching network for rectennas. *Sensors* **2017**, *17*, 1712.
6. Ripoll-Vercellone E.; Ferrandiz V.; Gasulla M. An add-on electronic device that upgrades mechanical gas meters into electronic ones. In Proceedings of the Eurosensors 2018, Graz, Austria, 9–12 September 2018.
7. Gutmann, R.J.; Borrego, J.M. Power Combining in an Array of Microwave Power Rectifiers. *IEEE Trans. Microw. Theory Tech.* **1979**, *27*, 958–968.
8. Reverter, F.; Gasulla, M. Optimal Inductor Current in Boost DC/DC Converters Regulating the Input Voltage Applied to Low-Power Photovoltaic Modules. *IEEE Trans. Power Electron.* **2017**, *32*, 6188–6196.



© 2018 by the authors. Licensee MDPI, Basel, Switzerland. This article is an open access article distributed under the terms and conditions of the Creative Commons Attribution (CC BY) license (<http://creativecommons.org/licenses/by/4.0/>).